

**Figure 4.** Beneficial effects of vandetanib on the survival time and the intrahepatic metastasis in mice implanted with KYN-2 cells. **A**, Kaplan-Meier estimates of survival in mice treated with vandetanib (75 mg/kg) compared with those treated with PBS. The survival time was counted from the day of tumor cell transplantation. \*,  $P < 0.05$ , compared with PBS-treated mice by log-rank test. **B**, numbers of tumor nodules in the liver were counted after 28 days of KYN-2 cells implantation and expressed as mean  $\pm$  SD ( $n = 6$  per group). \*,  $P < 0.05$ , compared with PBS-treated mice by Mann-Whitney  $U$  test.

## Discussion

In general, signal transduction through VEGFR-2 participates in endothelial cell proliferation much more than VEGFR-1 (20). Gule and colleagues (16) reported that the antitumor effects of vandetanib were mediated through inhibition of VEGF signaling and antiangiogenesis rather than through direct antiproliferative effects on tumor cells. In our *in vivo* study, vandetanib dose dependently suppressed the phosphorylation of VEGFR-2 and microvascular development. Furthermore, vandetanib also induced apoptosis of hepatoma cells *in vivo*, although it did not suppress the proliferation of hepatoma cells. O'Reilly and colleagues (21) reported that antiangiogenic therapy upregulated the apoptotic index of tumor cells but did not reduce the proliferation of tumor cells. The above results suggest that vandetanib mainly suppresses tumor growth through its tumor antiangiogenic effect by inhibition of VEGF signaling rather than suppressing the proliferation of tumor cells. In

our study, however, vandetanib at relatively high concentrations suppressed cell proliferation and increased apoptosis of hepatoma cells *in vitro*. In addition to EGF, fibroblast growth factor (FGF), and PDGF also participate in hepatoma cell proliferation (22, 23). At relatively high concentrations, vandetanib inhibits FGFR and PDGFR kinases (24). Because serum vandetanib levels were relatively high, high rate of apoptosis *in vivo* might be induced through inhibition of EGF and PDGF signaling, as well as FGF signaling. Thus, the inhibition of these signaling pathways seems important for the effects of vandetanib in the mouse HCC model, in addition to the inhibition of VEGF signaling.

In the orthotopic liver tumor xenograft model, which mirrors the clinical course of hepatoma more accurately than the subcutaneous xenograft model, serum vandetanib levels in 50- and 75 mg/kg-treated mice were not significantly different. However, tumor volume was significantly suppressed in a dose-dependent manner. In addition, vandetanib prolonged the survival time of tumor-bearing mice. It also suppressed the growth of larger HuH-7 xenografts. These findings suggest that vandetanib is potentially useful for patients with advanced HCCs. However, our study did

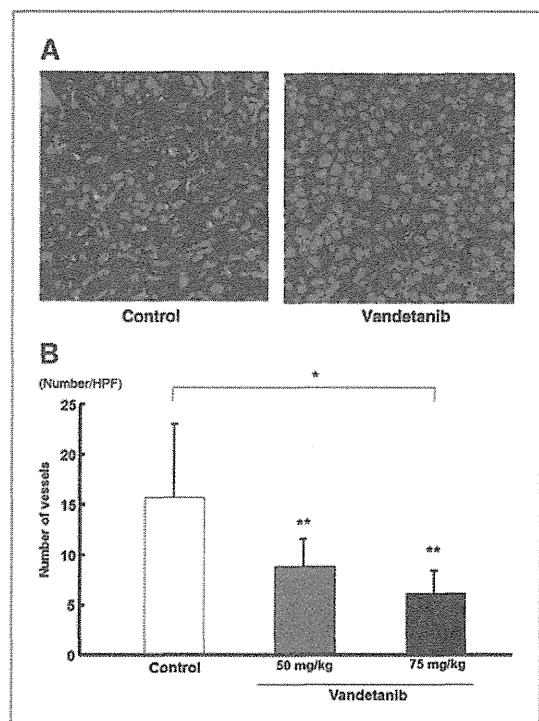


**Figure 5.** Effect of vandetanib on tumor vascularization. **A**, immunohistochemical analysis showed fewer CD31-positive vessels in tumor tissues of mice treated with vandetanib compared with the PBS-treated mice. **B**, the density of CD31-positive vessels in a tumor field is represented as mean  $\pm$  SD (50 fields of 18 sections from each of 6 tumors). \*,  $P < 0.05$ , compared with PBS-treated group by Kruskal-Wallis test; \*\*,  $P < 0.05$ , compared with PBS-treated group by Mann-Whitney  $U$  test.

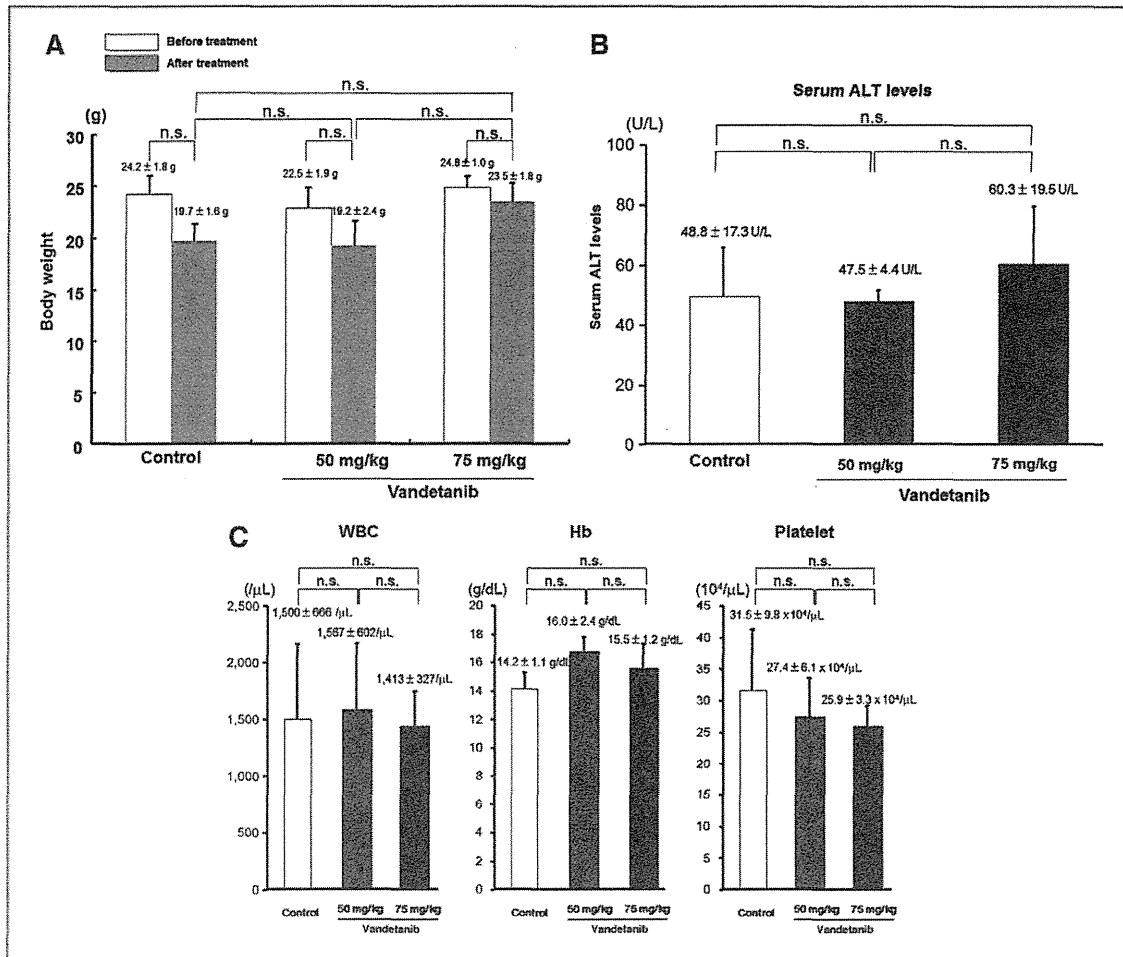


Figure 6. Effects of vandetanib on body weight, serum ALT levels, and bone marrow function in tumor-bearing mice. A, body weight of tumor-bearing mice in the PBS- and vandetanib-treated groups (50 and 75 mg/kg) at the start of treatment and at sacrifice. There was no significant difference in body weight between start of treatment and at sacrifice in each group. B, serum ALT levels in mice treated with PBS and vandetanib (50 and 75 mg/kg). C, leukocyte count, Hb level, and platelet count in PBS- and vandetanib-treated mice (50 and 75 mg/kg). Vandetanib did not result in any significant change in all 4 parameters. n.s., not significant; WBC, white blood cells.

not provide answers to why the antitumor effect of 75 mg/kg vandetanib was superior to that of 50 mg/kg even though the serum levels were not significantly different. Further studies of pharmacodynamics of vandetanib are needed.

Our results also showed that vandetanib significantly suppressed intrahepatic metastasis of KYN-2 cells. In their *in vitro* study, Giannelli and colleagues (25) reported that vandetanib blocked the proliferation, adhesion, migration, and invasion of hepatoma cells via inhibition of the EGFR pathway. Several studies have investigated tumor cell proliferation and metastasis (16, 25, 26), as well as the correlation between angiogenesis and tumor metastasis (27). What are the mechanisms of vandetanib-induced suppression of intrahepatic macrometastasis? While no direct mechanism was identified, our study showed 3 possible

mechanisms. First, vandetanib suppresses tumor cell migration from the primary tumor by inhibiting primary tumor growth and expansion. Second, vandetanib inhibits the EGFR pathway and thus suppresses the adhesion, migration, and invasion of hepatoma cells (28), which are critical steps in the metastatic process. Third, vandetanib inhibits metastatic tumor enlargement ensuring inactivity of micro-metastases (29).

Vandetanib administration did not reduce body weight, increase ALT, induce bone marrow suppression, or cause other serious adverse events. Recent clinical studies on the use of vandetanib in patients with lung cancer, the most common adverse events that resulted in discontinuation of vandetanib were diarrhea, rashes, and QTc prolongation (30). In the present study, we did not experience severe

diarrhea and skin rash in tumor-bearing nude mice. These differences could represent differences in species.

Several types of molecular-targeted agents are currently being investigated clinically. A recent study on advanced HCCs described the efficacy of the combination therapy of bevacizumab, a monoclonal antibody for VEGF-A, and erlotinib, which inhibits the phosphorylation of EGFR (31). The median survival period of patients on the combination therapy was 15.6 months and appeared favorable. The dual inhibition of VEGF and EGF signaling may be more effective in the treatment of HCCs. Several reports indicated that a larger EGFR gene copy number and the presence of EGFR mutation enhanced the therapeutic efficacy of EGFR inhibitors in lung cancer and metastatic colorectal cancer (32, 33). If such predictive markers are proved to be useful in HCCs, it will be easier to select patients with HCCs who will benefit most from vandetanib. In this study, we used xenograft HCC models and thus could not evaluate the influences of cirrhosis on treatment outcome. Such model might not precisely mirror the situation of human HCCs. Another investigation using HCC model with liver cirrhosis is required before any clinical application of vandetanib is possible.

In conclusion, we have shown in this study that vandetanib, a small-molecule tyrosine kinase inhibitor of VEGFR-2 and EGFR, significantly inhibited tumor growth and intrahepatic metastasis of hepatoma cells, had no serious

adverse events, and prolonged the survival time of tumor-bearing mice.

#### Disclosure of Potential Conflicts of Interest

M. Sata other entity (e.g., expert testimony) in MSD. No potential conflicts of interests were disclosed by the other authors.

#### Authors' Contributions

**Conception and design:** K. Inoue, T. Torimura, T. Nakamura, H. Masuda, O. Hashimoto, T. Ueno, M. Sata

**Development of methodology:** K. Inoue, T. Torimura, T. Nakamura, H. Masuda, M. Abe, O. Hashimoto, H. Koga, T. Ueno

**Acquisition of data (provided animals, acquired and managed patients, provided facilities, etc.):** K. Inoue, T. Torimura, T. Nakamura, H. Masuda, O. Hashimoto, H. Koga, T. Ueno, M. Sata

**Analysis and interpretation of data (e.g., statistical analysis, biostatistics, computational analysis):** K. Inoue, T. Torimura, T. Nakamura, H. Masuda, O. Hashimoto, H. Koga, T. Ueno, M. Sata

**Writing, review, and/or revision of the manuscript:** K. Inoue, T. Torimura, T. Nakamura, H. Masuda, O. Hashimoto, H. Koga, T. Ueno, M. Sata

**Administrative, technical, or material support (i.e., reporting or organizing data, constructing databases):** K. Inoue, T. Torimura, T. Nakamura, H. Iwamoto, H. Masuda, O. Hashimoto, T. Ueno, H. Yano

**Study supervision:** K. Inoue, T. Torimura, T. Nakamura, O. Hashimoto, T. Ueno, M. Sata

**Helped in K. Inoue's experiments:** H. Iwamoto

The costs of publication of this article were defrayed in part by the payment of page charges. This article must therefore be hereby marked *advertisement* in accordance with 18 U.S.C. Section 1734 solely to indicate this fact.

Received September 20, 2011; revised April 15, 2012; accepted May 11, 2012; published OnlineFirst May 18, 2012.

#### References

- Yang JD, Roberts LR. Hepatocellular carcinoma: a global view. *Nat Rev Gastroenterol Hepatol* 2010;7:448-58.
- Llovet JM, Ricci S, Mazzaferro V, Hilgard P, Gane E, Blanc JF, et al. Sorafenib in advanced hepatocellular carcinoma. *N Engl J Med* 2008;359:378-90.
- Llovet JM, Bruix J. Testing molecular therapies in hepatocellular carcinoma: the need for randomized phase II trials. *J Clin Oncol* 2009;27:833-5.
- Wilhelm SM, Carter C, Tang L, Wilkie D, McNabola A, Trail PA, et al. BAY 43-9006 exhibits broad spectrum oral antitumor activity and targets the RAF/MEK/ERK pathway and receptor tyrosine kinases involved in tumor progression and angiogenesis. *Cancer Res* 2004;64:7099-109.
- Strumberg D, Richly H, Hilger RA, Schleichner N, Korfee S, Tewes M, et al. Phase I clinical and pharmacokinetic study of the novel Raf kinase and vascular endothelial growth factor receptor inhibitor BAY 43-9006 in patients with advanced refractory solid tumors. *J Clin Oncol* 2005;23:965-72.
- Carlomagno F, Anaganti S, Guida T, Salvatore G, Troncone G, Wilhelm SM, et al. BAY 43-9006 inhibition of oncogenic RET mutants. *J Natl Cancer Inst* 2006;98:326-34.
- Kirsch M, Schackert G, Black PM. Metastasis and angiogenesis. *Cancer Treat Res* 2004;117:285-304.
- Geiger TR, Peeper DS. Metastasis mechanisms. *Biochim Biophys Acta* 2009;1793:293-308.
- Kudo M. Early detection and characterization of hepatocellular carcinoma: value of imaging multistep human hepatocarcinogenesis. *Intervirology* 2006;49:64-9.
- Miura H, Miyazaki T, Kuroda M, Oka T, Machinami R, Kodama T, et al. Increased expression of vascular endothelial growth factor in human hepatocellular carcinoma. *J Hepatol* 1997;27:854-61.
- Yamaguchi R, Yano H, Iemura A, Ogasawara S, Haramaki M, Kojiro M. Expression of vascular endothelial growth factor in human hepatocellular carcinoma. *Hepatology* 1998;28:68-77.
- Torimura T, Sata M, Ueno T, Kin M, Tsuji R, Sujaku K, et al. Increased expression of vascular endothelial growth factor is associated with tumor progression in hepatocellular carcinoma. *Hum Pathol* 1998;29:986-91.
- Borlak J, Meier T, Halter R, Spanel R, Spanel-Borowski K. Epidermal growth factor-induced hepatocellular carcinoma: gene expression profiles in precursor lesions, early stage and solitary tumours. *Oncogene* 2005;24:1809-19.
- Thorgeirsson SS, Grisham JW. Molecular pathogenesis of human hepatocellular carcinoma. *Nat Genet* 2002;31:339-46.
- Sagmeister S, Drucker C, Losert A, Grusch M, Daryabeigi A, Parzefall W, et al. HB-EGF is a paracrine growth stimulator for early tumor prestages in inflammation-associated hepatocarcinogenesis. *J Hepatol* 2008;49:955-64.
- Gule MK, Chen Y, Sano D, Frederick MJ, Zhou G, Zhao M, et al. Targeted therapy of VEGFR2 and EGFR significantly inhibits growth of anaplastic thyroid cancer in an orthotopic murine model. *Clin Cancer Res* 2011;62:4645-55.
- McCarty MF, Wey J, Stoelting O, Liu W, Fan F, Bucana C, et al. ZD6474, a vascular endothelial growth factor receptor tyrosine kinase inhibitor with additional activity against epidermal growth factor receptor tyrosine kinase, inhibits orthotopic growth and angiogenesis of gastric cancer. *Mol Cancer Ther* 2004;3:1041-8.
- Yano H, Maruiwa M, Murakami T, Fukuda K, Ito Y, Sugihara S, et al. A new human pleomorphic hepatocellular carcinoma cell line, KYN-2. *Acta Pathol Jpn* 1988;38:953-66.
- Yano H, Iemura A, Fukuda K, Mizoguchi A, Haramaki M, Kojiro M. Establishment of two distinct human hepatocellular carcinoma cell lines from a single nodule showing clonal dedifferentiation of cancer cells. *Hepatology* 1993;18:320-7.
- Takahashi T, Yamaguchi S, Chida K, Shibuya M. A single autophosphorylation site on KDR/FK-1 is essential for VEGF-A-dependent activation of PLC-gamma and DNA synthesis in vascular endothelial cells. *EMBO J* 2001;20:2768-78.

21. O'Reilly MS, Holmgren L, Shing Y, Chen C, Rosenthal RA, Moses M, et al. Angiostatin: a novel angiogenesis inhibitor that mediates the suppression of metastases by a Lewis lung carcinoma. *Cell* 1994;79:315-28.
22. Sasaki S, Ishida T, Toyota M, Ota A, Suzuki H, Ashida M, et al. Interferon- $\alpha/\beta$  and anti-fibroblast growth factor receptor 1 monoclonal antibody suppress hepatic cancer cells *in vitro* and *in vivo*. *PLoS One* 2011;6:e19618.
23. Stock P, Monga D, Tan X, Micsenyi A, Loizos N, Monga SP. Platelet-derived growth factor receptor alpha: a novel therapeutic target in human hepatocellular cancer. *Mol Cancer Ther* 2007;6:1932-41.
24. Wedge SR, Ogilvie DJ, Dukes M, Kendrew J, Chester R, Hennequin LF. ZD6474 inhibits vascular endothelial growth factor signaling, angiogenesis, and tumor growth following oral administration. *Cancer Res* 2002;62:4645-55.
25. Giannelli G, Azzariti A, Sgarra C, Porcelli L, Antonaci S, Paradiso A. ZD6474 inhibits proliferation and invasion of human hepatocellular carcinoma cells. *Biochem Pharmacol* 2006;71:479-85.
26. Arao T, Fukumoto H, Takeda M, Tamura T, Saijo N, Nishio K. Small in-frame deletion in the epidermal growth factor receptor as a target for ZD6474. *Cancer Res* 2004;64:9101-4.
27. Saaristo A, Karpanen T, Alitalo K. Mechanisms of angiogenesis and their use in the inhibition of tumor growth and metastasis. *Oncogene* 2000;19:6122-9.
28. Matsuo, Sakurai H, Saiki I. ZD1839, a selective epidermal growth factor receptor tyrosine kinase inhibitor, shows antimetastatic activity using a hepatocellular carcinoma model. *Mol Cancer Ther* 2003;2:557-61.
29. Holmgren L, O'Reilly MS, Folkman J. Dormancy of micrometastases: balanced proliferation and apoptosis in the presence of angiogenesis suppression. *Nat Med* 1995;1:149-53.
30. Natale RB, Badkin D, Govindan R, Sleckman GB, Rizvi NA, Capo A, et al. Vandetanib versus gefitinib in patients with advanced non-small-cell lung cancer: results from a two-part, double-blind, randomized phase II study. *J Clin Oncol* 2009;27:2523-9.
31. Thomas MB, Morris JS, Chadha R, Iwasaki M, Kaur H, Lin E, et al. phase II trial of the combination of bevacizumab and erlotinib in patients who have advanced hepatocellular carcinoma. *J Clin Oncol* 2009;27:843-50.
32. Linardou H, Dahabreh IJ, Kanaklopiti D, Siannis F, Bafaloukos D, Kosmidis P, et al. Assessment of somatic k-RAS mutations as a mechanism associated with resistance to EGFR-targeted agents: a systematic review and meta-analysis of studies in advanced non-small-cell lung cancer and metastatic colorectal cancer. *Lancet Oncol* 2008;9:962-72.
33. Gazdar AF. Personalized medicine and inhibition of EGFR signaling in lung cancer. *N Engl J Med* 2009;361:1018-20.

Original Article

# Hepatitis C virus core protein upregulates the expression of vascular endothelial growth factor via the nuclear factor- $\kappa$ B/hypoxia-inducible factor-1 $\alpha$ axis under hypoxic conditions

Mitsuhiko Abe,<sup>1</sup> Hironori Koga,<sup>1</sup> Takafumi Yoshida,<sup>1</sup> Hiroshi Masuda,<sup>1</sup> Hideki Iwamoto,<sup>1</sup> Masahiro Sakata,<sup>1</sup> Shinichiro Hanada,<sup>1</sup> Toru Nakamura,<sup>1</sup> Eitaro Taniguchi,<sup>1</sup> Takumi Kawaguchi,<sup>1</sup> Hirohisa Yano,<sup>2</sup> Takuji Torimura,<sup>3</sup> Takato Ueno<sup>4</sup> and Michio Sata<sup>1,3</sup>

<sup>1</sup>Division of Gastroenterology, Department of Medicine, <sup>2</sup>Department of Pathology, Kurume University School of Medicine, <sup>3</sup>Research Center for Innovative Cancer Therapy, Kurume University, Kurume and <sup>4</sup>Asakura Medical Association Hospital, Asakura, Japan

**Aim:** Hepatitis C virus (HCV) core protein critically contributes to hepatocarcinogenesis, which is often observed in liver cirrhosis. Since the liver cirrhosis microenvironment is affected by hypoxia, we focused on the possible driving force of HCV core protein on signal relay from hypoxia-inducible factor (HIF)-1 $\alpha$  to vascular endothelial growth factor (VEGF).

**Methods:** Human hepatocellular carcinoma cells stably overexpressing HCV core (Core cells) and NS5A (NS5A cells) were established; empty vector-transfected (EV) cells were used as controls. Hypoxia was induced by oxygen deprivation or by using cobalt chloride (CoCl<sub>2</sub>). YC-1 was used to inhibit HIF-1 $\alpha$  expression. Protein analyses for cultured cells and liver tissues obtained from CoCl<sub>2</sub>-treated HCV core-transgenic (Core-Tg) mice were performed by western blot and/or immunocytochemistry. Cellular mRNA levels were evaluated by quantitative real-time reverse transcription-polymerase chain reaction.

**Results:** Under hypoxia, the sustained expression of HIF-1 $\alpha$ , but not HIF-2 $\alpha$ , was profoundly observed in Core cells but, was faint in EV and NS5A cells. Immunocytochemistry revealed increased HIF-1 $\alpha$  in the nucleus. HIF-1 $\alpha$  mRNA levels were significantly higher in Core cells than in EV cells under both normoxia and hypoxia. The HIF-1 $\alpha$ -targeted VEGF and Bcl-xL expressions were increased in Core cells under hypoxia and abolished by YC-1 treatment. Hypoxic liver samples of Core-Tg mice indicated significant increases in both HIF-1 $\alpha$  and VEGF expression compared with the wild type.

**Conclusions:** Hepatitis C virus core protein has the distinct potential to transcriptionally upregulate and sustain HIF-1 $\alpha$  expression under hypoxia, thereby contributing to increased VEGF expression, a key regulator in the hypoxic milieu of liver cirrhosis.

**Key words:** hepatocellular carcinoma, hypoxia, transgenic mouse

## INTRODUCTION

HEPATITIS C VIRUS (HCV) is one of the major pathogens that cause chronic liver diseases, including liver cirrhosis; liver cirrhosis facilitates the develop-

ment of hepatocellular carcinoma (HCC) with an annual incidence of 7.9% in stage F4 liver cirrhosis.<sup>1</sup> Despite intensive research, the underlying mechanism of HCV-related HCC development remains unclear. Among HCV proteins, including structural (i.e., core, E1, E2, and p7) and nonstructural (i.e., NS2, NS3, NS4A, NS4B, NS5A, and NS5B) proteins, HCV core protein is suggested to play an important role in hepatocarcinogenesis.<sup>2</sup> Although the oncogenic effect of the protein on cellular DNA is unclear, its direct interaction with some transcription factors such as signal transducer and activator of transcription (STAT)3 and sterol

Correspondence: Dr Hironori Koga, Division of Gastroenterology, Department of Medicine, Kurume University School of Medicine, 67 Asahi-machi, Kurume 830-0011, Japan. Email: hirokoga@med.kurume-u.ac.jp

Received 1 October 2011; revision 17 November 2011; accepted 28 November 2011.

regulatory element-binding protein (SREBP)-1c are suggested to strongly promote and modulate the carcinogenesis process.<sup>3,4</sup>

In cirrhotic livers, blood supply is impaired as a consequence of fibrosis, which induces a hypoxic micro-environment in the liver.<sup>5</sup> Indeed, a previous study demonstrates that the expression level of hypoxia-inducible factor-1 $\alpha$  (HIF-1 $\alpha$ ), a nuclear transcription factor, gradually increases with the degree of fibrosis.<sup>6</sup> Under normoxic conditions, HIF-1 $\alpha$  is proline hydroxylated by HIF hydroxylase, resulting in degradation via the ubiquitin-proteasomal pathway, which involves von Hippel-Lindau (VHL) protein. In contrast, HIF-1 $\alpha$  is stabilized under hypoxia due to less hydroxylation; it reaches the nucleus, where it transactivates a variety of genes related to angiogenesis, glucose metabolism, cell proliferation, and anti-apoptosis.<sup>7</sup>

In this context, the mechanistic link between HCV infection and HIF-1 $\alpha$ -mediated cellular responses was recently examined.<sup>8,9</sup> It is reported that HCV upregulates the expression level of HIF-1 $\alpha$  protein, thereby leading to an increase in VEGF production and alterations to glucose metabolism.<sup>8,9</sup> However, it is not known which component protein of HCV is the main cause of HIF-1 $\alpha$  upregulation. Thus, the aim of the present study was to assess the possible involvement of HCV core protein in the hypoxic cellular responses, including angiogenesis, in comparison to NS5A protein, which is another potentially oncogenic viral component.<sup>10,11</sup>

## METHODS

### Materials

THE HIF-1A INHIBITOR, YC-1, was purchased from Sigma (St. Louis, MO, USA). The nuclear factor- $\kappa$ B (NF- $\kappa$ B) activation inhibitor, JSH-23, and the STAT3 inhibitor, S3I-201, were from Calbiochem (San Diego, CA, USA). The SPI inhibitor, mithramycin, was obtained from Santa Cruz Biotechnology (Santa Cruz, CA, USA). Cycloheximide was from Wako Pure Chemical Industries (Osaka, Japan). The primary antibodies used were directed against vascular endothelial growth factor (VEGF), Flk-1 (VEGFR2), and Lamin A/C (Santa Cruz Biotechnology); HIF-1 $\alpha$  (clone 54) (BD Biosciences, Franklin Lakes, NJ, USA); HIF-2 $\alpha$ , and HCV core (Abcam, Cambridge, MA, USA); p-VEGFR2 (Tyr1175), Bcl-xL, and c-Myc (Cell Signaling Technology, Beverly, MA, USA); FLAG (M2) and actin (Sigma); and c-myc tag antibody (Nacalai Tesque, Kyoto, Japan). Enhanced chemiluminescence reagents were obtained

from Amersham Pharmacia (Buckinghamshire, UK), and the protein assay reagents were from Bio-Rad (Hercules, CA, USA). All other reagents and compounds were of analytical grade.

### Cell lines and culture

Human hepatoma cell line HAK-1A and human umbilical vein endothelial cells (HUVECs) were used in this study. HAK-1A resembles well-differentiated HCC cells and was established from an HCV-related cirrhotic patient.<sup>12</sup> This cell line was grown in Dulbecco's modified Eagle medium (Wako Pure Chemical Industries) supplemented with 10% heat-inactivated (56°C for 30 min) fetal bovine serum (FBS) (BioWest, Nuaille, France), 100 units/mL penicillin, and 100  $\mu$ g/mL streptomycin (Nacalai Tesque) in a humidified atmosphere of 5% CO<sub>2</sub> at 37°C. HUVECs were purchased from Lonza (Walkersville, MD, USA) and cultured in EGM-2-based medium. Cell culturing under hypoxic conditions (1% oxygen) was performed using an APM-30D incubator with an oxygen concentration regulator system (ASTEC, Fukuoka, Japan). Alternatively, cells were exposed to the hypoxia-mimicking chemical cobalt chloride (CoCl<sub>2</sub>; Nacalai Tesque).<sup>13</sup>

### Transfection of cDNA and establishment of stable cell lines

The pcDNA3.1-based plasmid harboring HCV core cDNA (myc-tagged) was created as described previously.<sup>3</sup> The FLAG-tagged NS5A of the HCV (genotype 1b) expression plasmid was kindly provided by Dr Naoya Sakamoto (Tokyo Medical and Dental University, Japan). To generate stable transfectants, HAK-1A cells were transfected with HCV core, NS5A, or empty vector (EV) plasmid using the TransIT-LT1 Reagent (Mirus Bio Corporation, Madison, WI, USA), according to the manufacturer's instructions. HCV core-myc- and NS5A-FLAG-overexpressing clones as well as mock-transfected cells were selected by G418 (800  $\mu$ g/mL) and maintained in 400  $\mu$ g/mL of G418 (Nacalai Tesque).

### Western blot analysis

Cells were lysed in RIPA buffer (Pierce, Rockford, IL, USA) containing 1 mmol/L ethylenediaminetetraacetic acid (EDTA) (pH 8.0), 0.1 mmol/L sodium fluoride (NaF), 0.1 mmol/L sodium orthovanadate (Na<sub>3</sub>VO<sub>4</sub>), 100 mmol/L phenylmethylsulfonyl fluoride (PMSF), 1 mmol/L dithiothreitol (DTT), 2  $\times$  Protease Inhibitor

Cocktail (Nacalai Tesque), and 2  $\times$  Halt Phosphatase Inhibitor Cocktail (Pierce). The lysates were centrifuged at 19 300 g for 20 min at 4°C, and the supernatants were separated. For nuclear/cytoplasmic fractionation, NE-PER extraction reagent (Pierce) was used according to the manufacturer's protocol. Liver tissues obtained from mice were homogenized by a TissueLyser (Qiagen, Valencia, CA, USA) in cold lysis buffer, and the homogenates were clarified by centrifugation. Protein concentrations were measured using a Bio-Rad protein assay kit. After being boiled for 5 min in the presence of 2-mercaptoethanol, samples containing cell or tissue lysate proteins were separated on 8% or 10% sodium dodecyl sulfate (SDS)-polyacrylamide gels and subsequently transferred onto equilibrated polyvinylidene difluoride (PVDF) membranes (Bio-Rad). Proteins of the whole-cell lysates (35  $\mu$ g) as well as 25  $\mu$ g nuclear and 35  $\mu$ g cytoplasmic protein samples were applied to each lane on the gels. After masking by Protein-Free T20 (TBS) Blocking Buffer (Pierce), the membranes were incubated with the primary antibodies described above. The bound antibodies were detected with horseradish peroxidase (HRP)-labeled sheep anti-mouse IgG or HRP-labeled donkey anti-rabbit IgG (Amersham Pharmacia Biotech) using the enhanced chemiluminescence detection system (ECL Advanced kit). Positive signals from the target proteins were visualized using an image analyzer (LAS-4000; Fujifilm, Tokyo, Japan). Densitometry for the signals was performed using Multi Gauge version 3.0 software (Fujifilm).

### Immunofluorescence confocal laser scanning microscopy

Cells grown on 35-mm diameter glass-bottom dishes (MatTek, Ashland, MA, USA) were fixed with cold acetone/methanol (1:1) for 5 min, and subsequently washed in PBS containing 0.05% Tween 20 (PBS-T). Nonspecific reactions were blocked with Protein Block Serum-Free (DAKO North America, Carpinteria, CA, USA) and then incubated with anti-HIF-1 $\alpha$  antibody overnight at 4°C. After washing in PBS-T, the specimens were treated with Alexa Fluor goat anti-mouse IgG (H + L) antibody (Molecular Probes, Eugene, OR, USA) for 40 min at room temperature. Then, after their RNA was digested by RNase (Nippon Gene, Tokyo, Japan), the specimens were counterstained with propidium iodide (PI). A confocal laser scanning microscope (FLUOVIEW FV300; Olympus, Tokyo, Japan) equipped with an argon/krypton laser capable of dual

excitation and detection was used to observe the immunostaining for the protein and the nuclear localization of PI.

### Quantitative real-time RT-PCR

To analyze HIF-1 $\alpha$  and HIF-2 $\alpha$  mRNA expressions, total RNA was isolated from cells using TRIzol reagent (Invitrogen, Carlsbad, CA, USA). RNA was quantified by spectrophotometry. Real-time polymerase chain reaction (PCR) amplification was conducted using an ABI 7500 Real-Time PCR System instrument and software (Applied Biosystems, Tokyo, Japan). The following primer sets were used: GAPDH control forward: 5'-CATGAGAAGTATGACAACAGCC-3', GAPDH control reverse: 5'-AGTCCTTCCACGATACCAAAG-3'; HIF-1 $\alpha$  forward: 5'-TGCTCATCAGTTGCCACTTCC-3', HIF-1 $\alpha$  reverse: 5'-CCAAATCACCAGCATCCAGAAGT-3'; HIF-2 $\alpha$  forward: 5'-AGTGCATCATGTGTGTCAACTACG-3', HIF-2 $\alpha$  reverse: 5'-GGGCTGAACAGGGATTCAAGTC-3'. The PCR conditions and cycles were as follows: initial denaturation for 10 min at 95°C, followed by 40 cycles of denaturation at 95°C for 15 s and annealing/extension at 60°C for 60 s. Experiments were performed at least three times. The data are expressed as the fold changes of HCV core-overexpressing cells (Core cells) relative to mock-transfected cells (EV cells) using the Delta-Delta method. Relative gene expressions were normalized to that of GAPDH.

### Cell-cycle analysis by flow cytometry

DNA content was assessed by staining ethanol-fixed cells with PI and monitoring using a FACS Calibur (Becton Dickinson, Franklin Lakes, NJ, USA). The percentages of cells in the S, G<sub>0</sub>/G<sub>1</sub>, and G<sub>2</sub>/M phases of the cell cycle were determined using ModFit software (Verity Software House, Topsham, ME, USA).

### Cell proliferation assay

Cells (1  $\times$  10<sup>4</sup>) were seeded onto three wells in 6-well plates with or without 160  $\mu$ M CoCl<sub>2</sub>. After the cells were cultured for 8 days, the numbers of cells in 12 wells were counted in duplicate using a CDA-500 automated cell counter (Sysmex, Kobe, Japan).

### VEGFR2 phosphorylation assay

To examine if VEGF produced by the cells under hypoxic conditions was secreted into the culture media and biologically active, serum-free culture supernatants were collected from the CoCl<sub>2</sub>-treated cells and allowed to stimulate VEGFR2 in HUVECs for 10 min.

### HCV core-transgenic (Tg) mice and CoCl<sub>2</sub> treatment

The HCV core-Tg mice were kindly provided by Dr Takeshi Tokuhisa (Chiba University, Japan). To determine the possible driving force of HCV core protein on the HIF-1 $\alpha$ /VEGF axis *in vivo*, 16-week-old male Core-Tg mice (Core-Tg) and wild-type control mice (Wild) were given a single intraperitoneal injection of CoCl<sub>2</sub> at 60  $\mu$ g/g body weight and killed 6 h later as described previously.<sup>14,15</sup> Liver tissues were subjected to western blot analysis. All animal experiments were conducted in accordance with the NIH Guidelines for the Care and Use of Laboratory Animals and were approved by the University of Kurume Institutional Animal Care and Use Committee.

### Statistical analysis

Statistical significance was assessed using the Mann-Whitney *U*-test. *P* < 0.05 was considered statistically significant.

## RESULTS

### HCV core enhances the hypoxia-induced expression of HIF-1 $\alpha$ protein

WE ESTABLISHED HAK-1A-BASED cell clones stably overexpressing HCV core protein (Core cells) and NS5A protein (NS cells) (Fig. 1a). Stable transfectants with empty vector plasmid cDNA (EV cells) were used as controls. When Core and EV cells were exposed to 1% O<sub>2</sub> for 6 h, Core cells expressed more HIF-1 $\alpha$  than EV cells did, although only a slight increase in HIF-2 $\alpha$  expression was observed in Core cells (Fig. 1b). Since HIF- $\alpha$  proteins, including HIF-1 $\alpha$ , are transcription factors and are known to function in the nucleus, we confirmed the nuclear localization of HIF-1 $\alpha$  under hypoxic conditions by immunocytochemistry using 160  $\mu$ M CoCl<sub>2</sub> (Fig. 1c). Furthermore, western blot analysis in combination with nuclear/cytoplasmic fractionation was used to strengthen the predominant nuclear upregulation of HIF-1 $\alpha$  in Core cells under hypoxic conditions (Fig. 1d). It was evident that nuclear upregulation in hypoxic Core cells was unique to HIF-1 $\alpha$  and not HIF-2 $\alpha$ . Next, we tested if other HCV-derived proteins including NS5A, which is also suggested to have oncogenic potential like HCV core protein,<sup>10,11</sup> exhibited similar effects. However, NS5A overexpression under hypoxic conditions caused no clear increase in HIF-1 $\alpha$  (Fig. 1e).

### HIF-1 $\alpha$ degradation was not retarded in Core cells

The intracellular amount of HIF-1 $\alpha$  is balanced between its production and degradation; degradation is tightly regulated by the ubiquitin-proteasomal pathway. Thus, to examine initially whether HCV core upregulates the expression level of HIF-1 $\alpha$  by directly inhibiting the degradation pathway, we chased the protein expression levels after inhibiting protein synthesis using cycloheximide (CHX) under hypoxic conditions. HIF-1 $\alpha$  expression levels decreased 30 and 60 min after treating cells with 5  $\mu$ g/mL CHX to 36% and 65% in EV cells and 42% and 60% in Core cells, respectively. These results suggest that the degradation efficiency of the protein is not lowered by HCV core protein (Fig. 2).

### HCV core transcriptionally upregulated HIF-1 $\alpha$ expression

To investigate whether HIF-1 $\alpha$  is transcriptionally upregulated in Core cells, we performed quantitative real-time reverse transcription (RT)-PCR to measure HIF-1 $\alpha$  mRNA levels. The transcriptional levels of HIF-1 $\alpha$  in Core cells were significantly higher than those in EV cells under both normoxic and hypoxic conditions. Consistent with the protein analysis results in this study, the transcriptional levels of HIF-2 $\alpha$  were not significantly different between Core and EV cells (Fig. 3a). Since recent data suggest that distinct transcription factors such as NF- $\kappa$ B, SP-1, and STAT3 directly control HIF-1 $\alpha$  mRNA synthesis,<sup>16–19</sup> we explored which factor(s) contributed most to the upregulation of HIF-1 $\alpha$  by using specific inhibitors against these three transcription factors. Under hypoxic conditions, the upregulated HIF-1 $\alpha$  protein expression in Core cells was suppressed by the NF- $\kappa$ B activation inhibitor, JSH-23 (30  $\mu$ M), but not by the SP-1 inhibitor, mithramycin (100 nM), or the STAT3 inhibitor, S3I-201 (100  $\mu$ M) (Fig. 3b). When the concentration of JSH-23 was increased to 60  $\mu$ M under hypoxic conditions, the upregulated HIF-1 $\alpha$  protein expression was clearly abolished in concert with the decreased expression of NF- $\kappa$ B (Fig. 3c). These findings strongly suggest that HCV core elevates the mRNA expression levels of HIF-1 $\alpha$  by activating the NF- $\kappa$ B signaling pathway.

### HCV core-induced HIF-1 $\alpha$ increased VEGF expression under hypoxia

Since HIF-1 $\alpha$  regulates a diverse range of cellular events, including cell proliferation, angiogenesis, and



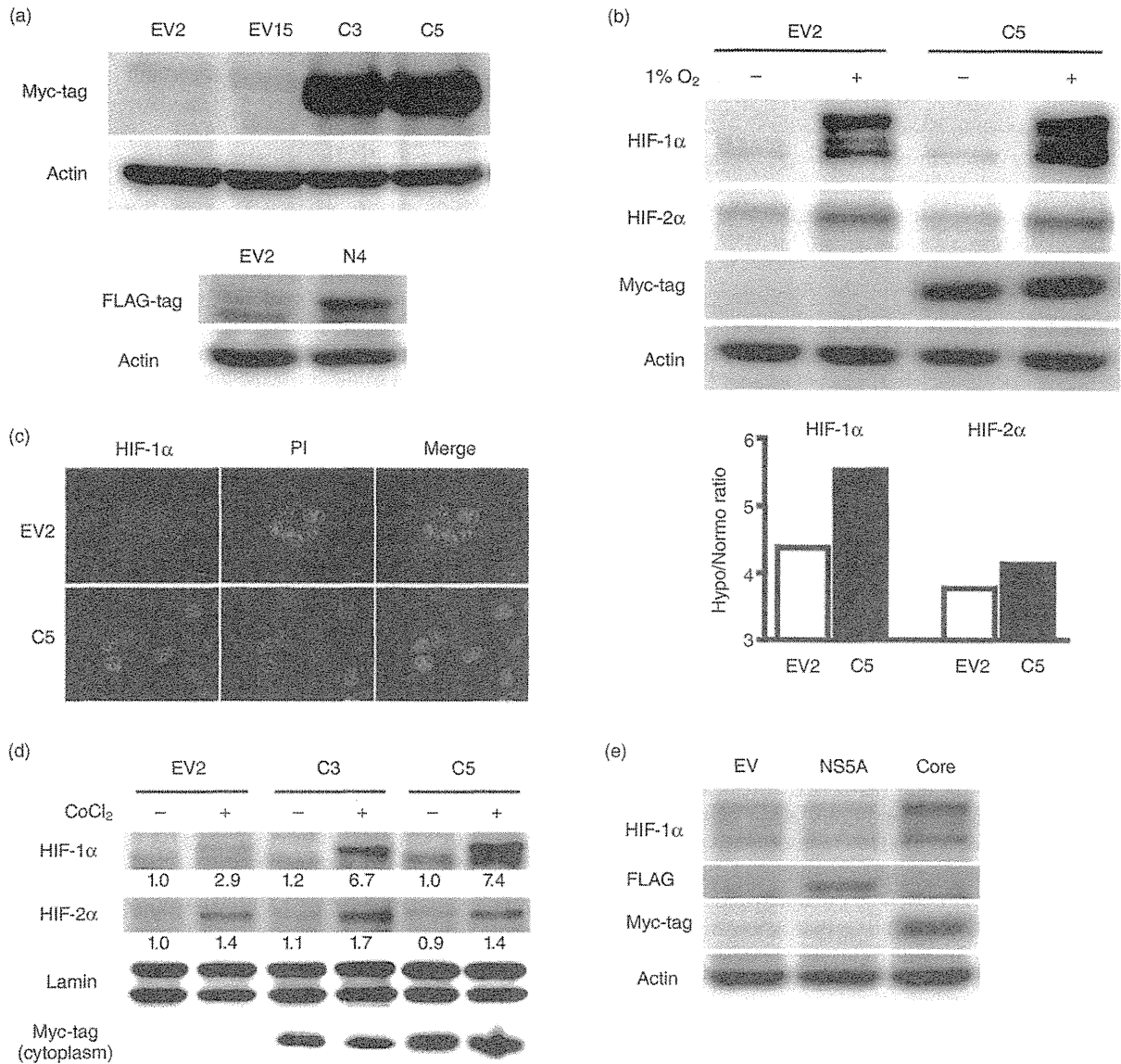


**Figure 1** Preferential induction of hypoxia-inducible factor (HIF)-1 $\alpha$  via hepatitis C virus (HCV) core under hypoxia. (a) Western blot analysis of stable cell lines. Positive signals for Myc-tag (HCV core) and FLAG-tag (HCV NS5A) are shown in clones C3 and C5, and N4, respectively. EV2 and EV15, empty vector (EV)-transfected HAK-1A cell clones 2 and 15. (b) EV2 and C5 were exposed to 20% and 1% O<sub>2</sub> for 6 h, respectively. The protein expression levels of HIF-1 $\alpha$  and HIF-2 $\alpha$  were examined by western blot analysis. Protein (35  $\mu$ g) of whole-cell lysates was applied to each lane. Lower graph shows densitometric ratios of HIF protein expressions under hypoxia (Hypo) to those under normoxia (Normo). (c) Confocal laser scanning microscopy for the nuclear localization of HIF-1 $\alpha$  protein under hypoxic conditions. (d) EV2, C3, and C5 cells were treated with or without 160  $\mu$ M CoCl<sub>2</sub> for 24 h, and their nuclear extracts were subjected to western blot analysis for HIF-1 $\alpha$  and HIF-2 $\alpha$ . Lamin A/C (Lamin) was used as a control protein to monitor valid nuclear/cytoplasmic fractionation. Relative densitometric values for HIF-1 $\alpha$  and HIF-2 $\alpha$  expression levels are presented beneath the corresponding bands. (e) Comparison of HIF-1 $\alpha$  protein expression levels among EV (EV2), NS5A (N4), and Core (C5) cells by western blot analysis. Whole-cell lysates from the cells exposed to 160  $\mu$ M CoCl<sub>2</sub> for 24 h were used.

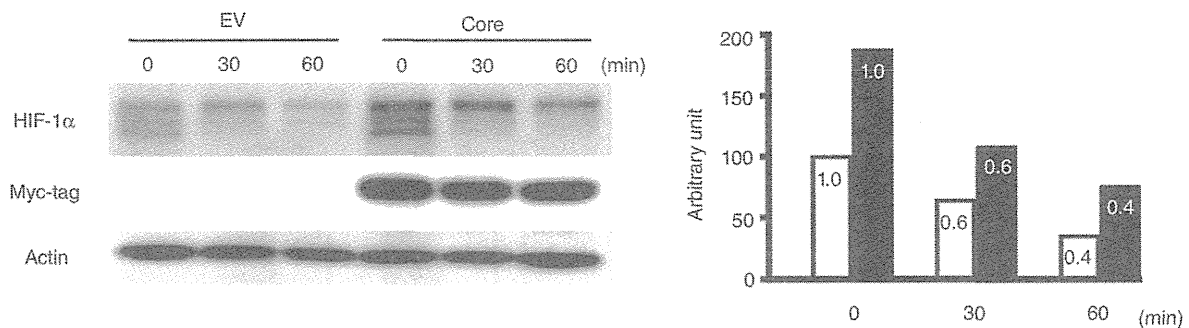


**Figure 2** Hepatitis C virus (HCV) core does not promote hypoxia-inducible factor (HIF)-1 $\alpha$  degradation. EV (EV2) and Core (C5) were exposed to 5  $\mu$ g/mL cycloheximide (CHX) for 0, 30, or 60 min at the last phase of the 24-h CoCl<sub>2</sub> treatment. Whole-cell lysates were used for western blot analysis to evaluate HIF-1 $\alpha$  expression levels after protein synthesis was inhibited by CHX administration. Right panel shows densitometric values (time 0 = 1.0) for the HIF-1 $\alpha$  expression levels. □, EV; ■, Core.

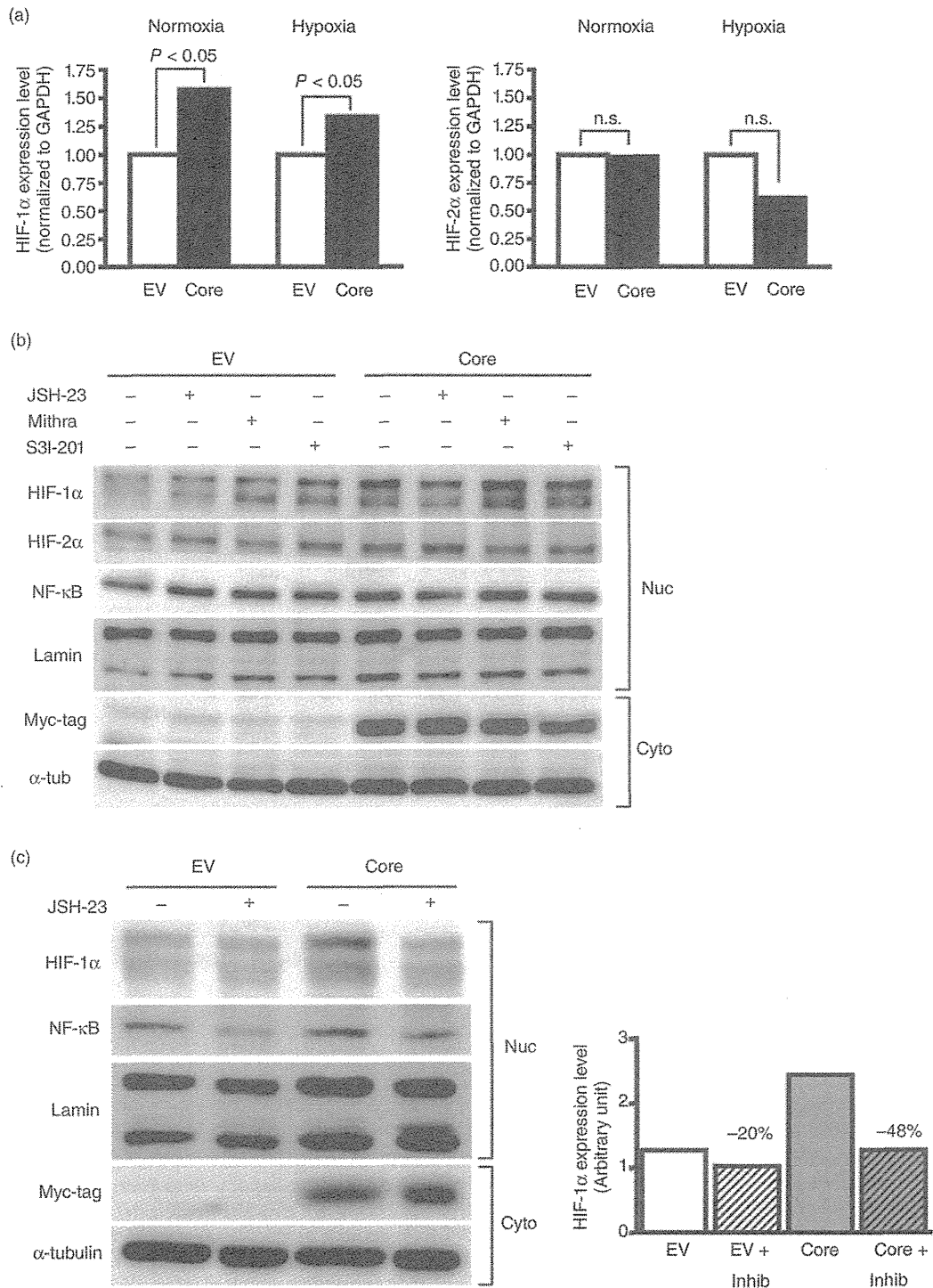
anti-apoptosis, the net effects resulting from increased intracellular HIF-1 $\alpha$  were compared between Core and EV cells. In cell cycle analyses, Core cells exhibited a slight decrease in the number of cells in the S phase compared with EV cells under hypoxia; however, Core cells also demonstrated a similar increase under normoxia (Fig. 4a). This finding led to a similar but significant difference in the actual cell number at culture day 8 (Fig. 4b). Taken together, these results suggest that HCV core-induced HIF-1 $\alpha$  expression under hypoxia confers anti-proliferative activity to liver cancer cells. Next, we evaluated if VEGF and Bcl-xL are upregulated in Core cells under hypoxic conditions, since they are downstream gene products of HIF-1 $\alpha$ . As expected, the expression levels of both proteins were elevated in Core cells under hypoxia, followed by the upregulation of HIF-1 $\alpha$  (Fig. 4c). It is worth noting that when the cells were incubated with the HIF-1 $\alpha$  inhibitor, YC-1 (10  $\mu$ M), the elevations in VEGF and Bcl-xL expression were clearly abolished according to the diminished HIF-1 $\alpha$  expression; this suggests that the induced HIF-1 $\alpha$  plays roles in

angiogenesis and anti-apoptosis in Core cells under hypoxia (Fig. 4c). To assess whether VEGF produced by the Core cells was secreted into the culture media and if it was biologically functional, whether the supernatants of the cells caused VEGFR2 phosphorylation in HUVECs was tested. Only the supernatants from Core cells induced clear VEGFR2 phosphorylation at Tyr<sup>1175</sup>, which is a hallmark of the activation of the VEGFR signaling pathway (Fig. 4d). On the other hand, supernatants from EV and NS5A cells failed to increase the Tyr<sup>1175</sup>-phosphorylated VEGFR2 protein expression in HUVECs (Fig. 4d).

#### Predominant induction of HIF-1 $\alpha$ expression in HCV core-transgenic mice

To determine whether HCV core-related HIF-1 $\alpha$  upregulation really occurs in hypoxic livers, protein extracts were obtained from the livers of Core-Tg and Wild mice that received equal treatment with intraperitoneal CoCl<sub>2</sub>. Although there were slight variations in the expression levels in HIF-1 $\alpha$  and VEGF among the

**Figure 3** Involvement of nuclear factor- $\kappa$ B (NF- $\kappa$ B) in the hepatitis C virus (HCV) core-mediated hypoxia-inducible factor (HIF)-1 $\alpha$  upregulation. (a) Quantitative real-time reverse transcription-polymerase chain reaction (RT-PCR) analysis for HIF-1 $\alpha$  and HIF-2 $\alpha$  mRNA expression levels. Total RNA was extracted from EV (EV2) and Core (C5) cells 24 h after 160  $\mu$ M CoCl<sub>2</sub> treatment. The RT-PCR products of glyceraldehyde 3-phosphate dehydrogenase (GAPDH) were chosen as an internal standard for RNA quantity and integrity. Ratios of HIF-1 $\alpha$  and HIF-2 $\alpha$  mRNA levels to those of GAPDH are expressed as mean (SD) ( $n = 6$ ). n.s., not significant. (b) EV and Core cells were treated with JSH-23 (30  $\mu$ M), mithramycin (100 nM), or S3I-201 (100  $\mu$ M) for 24 h under CoCl<sub>2</sub>-induced hypoxic conditions. Nuclear extracts obtained from the cells were subjected to western blot analysis for the indicated molecules. (c) NF- $\kappa$ B expression level was suppressed in the Core cells treated with 60  $\mu$ M JSH-23. Nuclear extracts of the cells were used for western blot analysis. Densitometry results regarding HIF-1 $\alpha$  band intensity are presented (right panel). Percentages are decreased rates in the densitometric values after JSH-23 treatment. Nuc, nuclear; Cyto, cytoplasmic; Inhib, inhibitor (JSH-23).



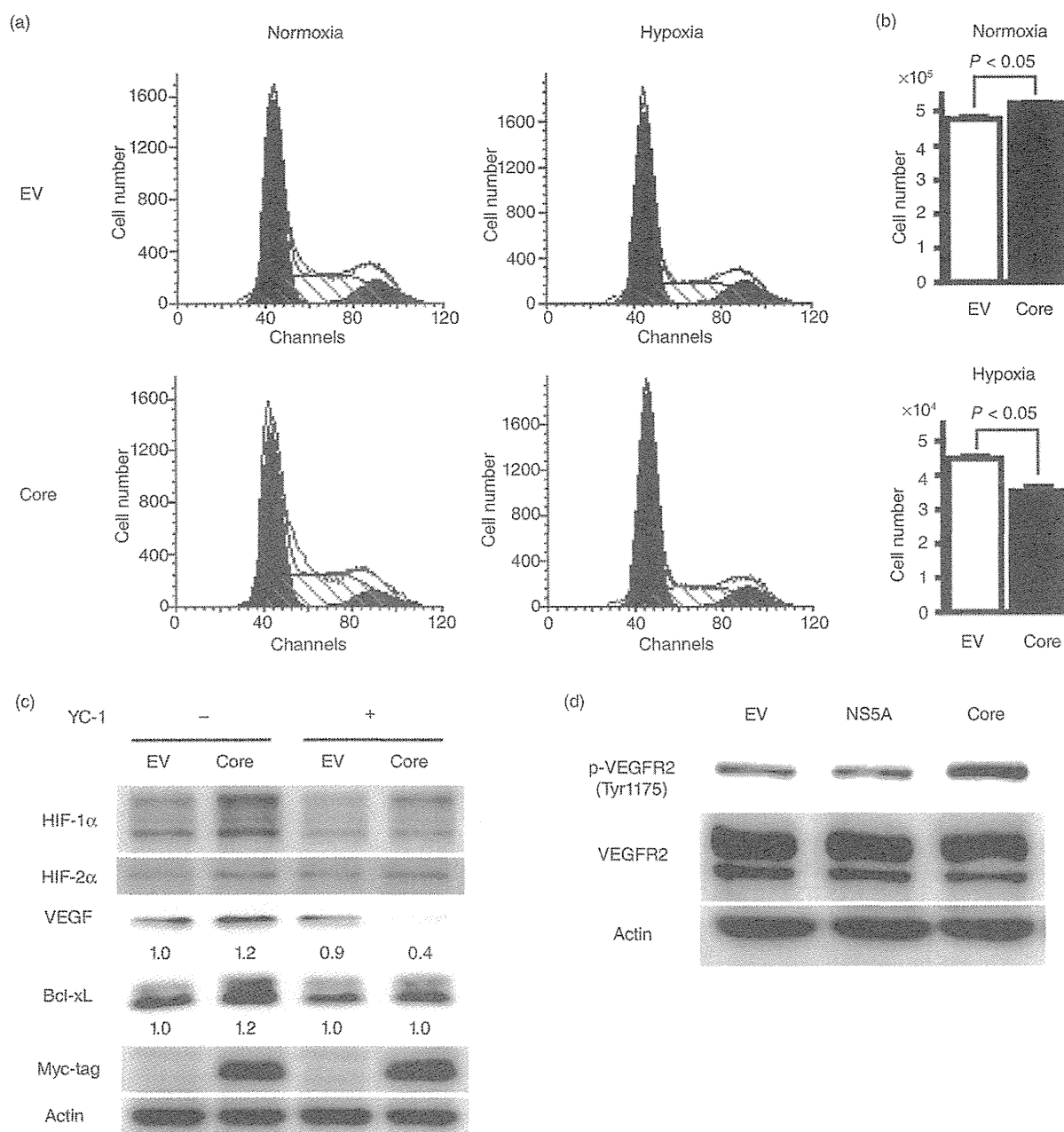


**Figure 4** Increased functional vascular endothelial growth factor (VEGF) production in Core cells under hypoxia. (a) Flow cytometric analysis of the cell cycle in EV (EV2) and Core (C5) cells treated with (hypoxia) or without (normoxia) 160  $\mu\text{M}$   $\text{CoCl}_2$  for 24 h. (b) Machine-counted numbers of EV and Core cells with or without  $\text{CoCl}_2$  8 days after seeding. (c) Western blot analysis focusing on the expression levels of hypoxia-inducible factor (HIF)-1 $\alpha$  target gene products such as VEGF and Bcl-xL. Cells were treated with or without 10  $\mu\text{M}$  YC-1 for 10 h under the  $\text{CoCl}_2$ -induced hypoxic conditions. Relative densitometric values for VEGF and Bcl-xL expression levels are presented beneath the corresponding bands. (d) Human umbilical vein endothelial cells (HUVECs) were cultured in serum-free spent media obtained from culture dishes for EV (EV2), NS5A (N4), and Core (C5) cells. The expression levels of Tyr<sup>1175</sup>-phosphorylated (p-) VEGFR2 and total VEGFR2 were evaluated by western blot analysis.

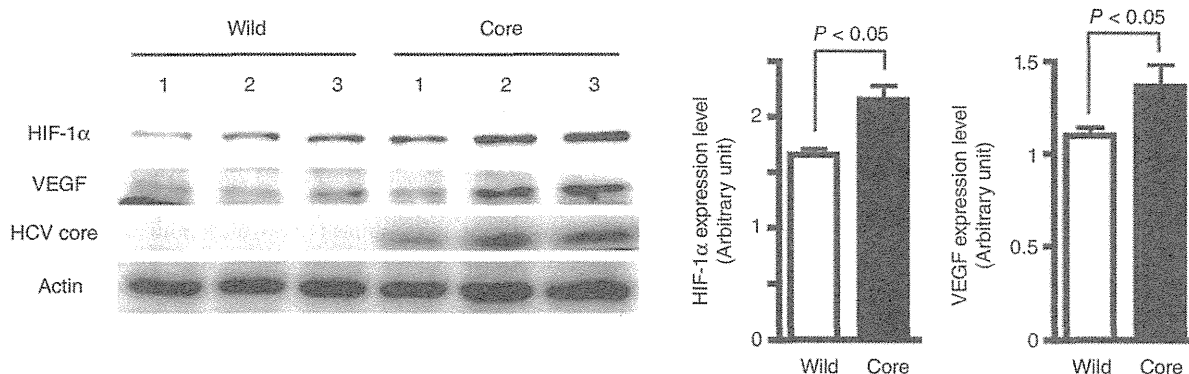


**Figure 5** Comparison of the expression levels of hypoxia-inducible factor (HIF)-1 $\alpha$  and vascular endothelial growth factor (VEGF) between wild-type (Wild) and Core-Tg (Core) mice treated with an intraperitoneal injection of CoCl<sub>2</sub> (60  $\mu$ g/g body weight). The mice were killed 6 h after injection. Protein extracts from the liver tissues were subjected to western blot analysis. Densitometric analysis of visualized bands for HIF-1 $\alpha$  and VEGF was performed.

animals in each group, both protein levels were significantly higher in Core-Tg than in Wild mice after CoCl<sub>2</sub> administration (Fig. 5). These findings suggest that the HCV core-involved hypoxic response is universal, even *in vivo*.

## DISCUSSION

THE RESULTS OF the present study demonstrate the following: (i) HCV core protein preferentially induces high expression levels of HIF-1 $\alpha$  protein in hepatocyte-derived cells under hypoxic conditions; (ii) NF- $\kappa$ B-mediated transcriptional upregulation but not attenuated protein degradation contributes to the HIF-1 $\alpha$  expression augmented by HCV core protein; (iii) one of the important biological consequences of the increased HIF-1 $\alpha$  is the production of active VEGF, which leads to VEGFR2 activation in endothelial cells; and (iv) the hypoxic livers of Core-Tg mice exhibit significantly higher HIF-1 $\alpha$  expression levels.

Previous studies suggest that HCV plays a role in upregulating HIF-1 $\alpha$  expression,<sup>8,9</sup> however, these studies do not focus on the involvement of specific HCV proteins involved in HIF-1 $\alpha$  upregulation. On this point, the present study demonstrates that HCV core is responsible for the upregulation of HIF-1 $\alpha$ . Furthermore, the expression mode of HIF-1 $\alpha$  protein differs between the previous and present reports, in that the HCV-related HIF-1 $\alpha$  increase was observed even under normoxia in the previous reports but, strictly under hypoxia in the present report. This discrepancy might be derived from differences in HCV-related materials

and/or the cell lines used. In the present study, it is worth noting that NS5A, another potentially oncogenic protein of HCV,<sup>10,11</sup> did not induce HIF-1 $\alpha$  upregulation under hypoxia, suggesting that HCV core protein contributes more to hepatocarcinogenesis under hypoxia via angiogenesis, a fundamental biological event in the microenvironment of cirrhotic liver.<sup>5,6</sup>

Our results suggest that the HCV core/NF- $\kappa$ B axis plays a significant role in HIF-1 $\alpha$  augmentation. The role of this axis seems reasonable, since it is known that HCV core activates NF- $\kappa$ B in several other cell systems.<sup>20,21</sup> Other transcription factors known to upregulate HIF-1 $\alpha$ , such as SP-1 and STAT3, were not involved in the HCV core-augmented HIF-1 $\alpha$  expression under hypoxia in this study. Determining the detailed mechanism of the distinct collaborative role of NF- $\kappa$ B and HCV core in upregulating HIF-1 $\alpha$  requires further investigation.

Among the HIF-1 $\alpha$ -regulated diverse cellular events, including angiogenesis, proliferation, apoptosis/survival, and metabolism, angiogenesis was found to be a major biological output in Core cells under hypoxia. Indeed, the results of this study demonstrate that HCV core-induced HIF-1 $\alpha$  activates the VEGFR2 signaling pathway in endothelial cells via VEGF secreted by the Core cells under hypoxic conditions. The distinct angiogenic potential of HCV core protein under hypoxia might help transformed cells survive in the hypoxic milieu of the cirrhotic liver by supplying them with oxygen and nutrients. HCV is known to be able to replicate in HCC tissue;<sup>22</sup> however, the viral load is estimated to be lower than that in surrounding noncan-

cerous liver tissue.<sup>23</sup> Thus, the virus-derived angiogenic drive is thought to be less pronounced in overt HCC than in noncancerous livers. Indeed, clinical data supporting the predominant upregulation of VEGF in patients infected with HCV as compared with those infected with HBV are unavailable.

Taken together, it can be speculated that preventing the inflammation and subsequent fibrosis caused by persistent HCV infection is crucial to suppressing the hypoxia-mediated oncogenic pressure on HCV core-harboring hepatocytes.

#### ACKNOWLEDGMENTS

WE THANK DR Reichiro Kuwahara and Ms Mari Hagiwara for technical assistance in handling mouse liver tissues.

#### REFERENCES

- 1 Yoshida H, Shiratori Y, Moriyama M *et al.* Interferon therapy reduces the risk for hepatocellular carcinoma: national surveillance program of cirrhotic and noncirrhotic patients with chronic hepatitis C in Japan. IHIT Study Group. Inhibition of Hepatocarcinogenesis by Interferon Therapy. *Ann Intern Med* 1999; 131: 174–81.
- 2 Moriya K, Fujie H, Shintani Y *et al.* The core protein of hepatitis C virus induces hepatocellular carcinoma in transgenic mice. *Nat Med* 1998; 4: 1065–7.
- 3 Yoshida T, Hanada T, Tokuhisa T *et al.* Activation of STAT3 by the hepatitis C virus core protein leads to cellular transformation. *J Exp Med* 2002; 196: 641–53.
- 4 Moriishi K, Mochizuki R, Moriya K *et al.* Critical role of PA28 $\gamma$  in hepatitis C virus-associated steatogenesis and hepatocarcinogenesis. *Proc Natl Acad Sci U S A* 2007; 104: 1661–6.
- 5 Kim KR, Moon HE, Kim KW. Hypoxia-induced angiogenesis in human hepatocellular carcinoma. *J Mol Med (Berlin)* 2002; 80: 703–14.
- 6 Bozova S, Elpek GO. Hypoxia-inducible factor-1 $\alpha$  expression in experimental cirrhosis: correlation with vascular endothelial growth factor expression and angiogenesis. *APMIS* 2007; 115: 795–801.
- 7 Majmundar AJ, Wong WJ, Simon MC. Hypoxia-inducible factors and the response to hypoxic stress. *Mol Cell* 2010; 40: 294–309.
- 8 Nasimuzzaman M, Waris G, Mikolon D, Stupack DG, Siddiqui A. Hepatitis C virus stabilizes hypoxia-inducible factor 1 $\alpha$  and stimulates the synthesis of vascular endothelial growth factor. *J Virol* 2007; 81: 10249–57.
- 9 Ripoli M, D'Aprile A, Quarato G *et al.* Hepatitis C virus-linked mitochondrial dysfunction promotes hypoxia-inducible factor 1 $\alpha$ -mediated glycolytic adaptation. *J Virol* 2010; 84: 647–60.
- 10 Park CY, Choi SH, Kang SM *et al.* Nonstructural 5A protein activates  $\beta$ -catenin signaling cascades: implication of hepatitis C virus-induced liver pathogenesis. *J Hepatol* 2009; 51: 853–64.
- 11 Wang AG, Lee DS, Moon HB *et al.* Non-structural 5A protein of hepatitis C virus induces a range of liver pathology in transgenic mice. *J Pathol* 2009; 219: 253–62.
- 12 Yano H, Iemura A, Fukuda K, Mizoguchi A, Haramaki M, Kojiro M. Establishment of two distinct human hepatocellular carcinoma cell lines from a single nodule showing clonal dedifferentiation of cancer cells. *Hepatology* 1993; 18: 320–7.
- 13 Wang GL, Semenza GL. General involvement of hypoxia-inducible factor 1 in transcriptional response to hypoxia. *Proc Natl Acad Sci U S A* 1993; 90: 4304–8.
- 14 Bergeron M, Gidday JM, Yu AY, Semenza GL, Ferrero DM, Sharp FR. Role of hypoxia-inducible factor-1 in hypoxia-induced ischemic tolerance in neonatal rat brain. *Ann Neurol* 2000; 48: 285–96.
- 15 Todorov V, Gess B, Gödecke A, Wagner C, Schröder J, Kurtz A. Endogenous nitric oxide attenuates erythropoietin gene expression in vivo. *Pflugers Arch* 2000; 439: 445–8.
- 16 Papadakis AI, Paraskeva E, Peidis P *et al.* eIF2 $\alpha$  Kinase PKR modulates the hypoxic response by Stat3-dependent transcriptional suppression of HIF-1 $\alpha$ . *Cancer Res* 2010; 70: 7820–9.
- 17 Rius J, Guma M, Schachtrup C *et al.* NF- $\kappa$ B links innate immunity to the hypoxic response through transcriptional regulation of HIF-1 $\alpha$ . *Nature* 2008; 453: 807–11.
- 18 Vlamincck B, Toffoli S, Ghislain B, Demazy C, Raes M, Michiels C. Dual effect of echinomycin on hypoxia-inducible factor-1 activity under normoxic and hypoxic conditions. *FEBS J* 2007; 274: 5533–42.
- 19 Niu G, Briggs J, Deng J *et al.* Signal transducer and activator of transcription 3 is required for hypoxia-inducible factor-1 $\alpha$  RNA expression in both tumor cells and tumor-associated myeloid cells. *Mol Cancer Res* 2008; 6: 1099–105.
- 20 Sato Y, Kato J, Takimoto R *et al.* Hepatitis C virus core protein promotes proliferation of human hepatoma cells through enhancement of transforming growth factor  $\alpha$  expression via activation of nuclear factor- $\kappa$ B. *Gut* 2006; 55: 1801–8.
- 21 Yoshida H, Kato N, Shiratori Y *et al.* Hepatitis C virus core protein activates nuclear factor  $\kappa$ B-dependent signaling through tumor necrosis factor receptor-associated factor. *J Biol Chem* 2001; 276: 16399–405.
- 22 Ohishi M, Sakisaka S, Harada M *et al.* Detection of hepatitis-C virus and hepatitis-C virus replication in hepatocellular carcinoma by in situ hybridization. *Scand J Gastroenterol* 1999; 34: 432–8.
- 23 Tang L, Tanaka Y, Enomoto N, Marumo F, Sato C. Detection of hepatitis C virus RNA in hepatocellular carcinoma by in situ hybridization. *Cancer* 1995; 76: 2211–16.

